Interference Rejection Techniques in Spread Spectrum Communications

LAURENCE B. MILSTEIN, FELLOW, IEEE

Invited Paper

Spread spectrum communication systems have many applications, including interference rejection, multiple accessing, multipath suppression, low probability of intercept transmission, and accurate ranging. Of all the potential applications, the ability of a spread spectrum system to withstand interference, both intentional and unintentional, is probably its greatest asset. Of course, any spread spectrum receiver can only suppress a given amount of interference; if the level of interference becomes too great, the system will not function properly.

Even under these latter circumstances, however, other techniques, which enhance the performance of the system over and above the performance improvement that comes automatically to systems simply by employing spread spectrum, are available for use. These techniques typically involve some type of additional signal processing and are the subject of this paper. In particular, two general types of narrow-band interference suppression schemes are discussed in depth, and a short overview is presented for several other techniques as well. The two classes of rejection schemes emphasized in the paper are 1) those based upon least-mean square estimation techniques, and 2) those based upon transform domain processing structures.

I. INTRODUCTION

The most important use of a spread spectrum communication system is that of interference suppression. As is well known [41], [42], [49], [53], the inherent processing gain of a spread spectrum system will, in many cases, provide the system with a sufficient degree of interference rejection capability. However, at times the interfering signal is powerful enough so that even with the advantage that the system obtains by spreading the spectrum, communication becomes effectively impossible. In some of these cases, the interference immunity can be improved significantly by using signal processing techniques which complement the spread spectrum modulation.

From basic detection theory [16], [42], [54], the optimal receiver for detecting a known signal in additive white

gaussian noise (AWGN) consists of a parallel bank of matched filters, where the number of such filters is determined by the dimensionality of the signal set. For binary antipodal signaling (i.e., a system wherein two signals are used, say, $s_1(t)$ and $s_2(t)$, such that $s_1(t) = -s_2(t)$), only a single matched filter is required. Since a correlation receiver is equivalent to a matched filter receiver, a receiver that performs a single coherent correlation is optimum for detecting one of two known antipodal waveforms.

If the noise is gaussian but not white, the receiver is much more complex, and indeed requires the solution of an integral equation to fully specify it. However, under the special condition of an infinite observation interval, the form of the optimal receiver reduces to the cascade of a prewhitening filter and a matched filter, where the transfer function of the prewhitening filter is the inverse of the power spectral density of the noise, and the matched filter is again matched to the signal structure.

When the signal is being received in nongaussian noise, the situation becomes even more difficult. For the special case of a signal embedded in noise plus sine-wave interference, a nonlinear receiver was shown in [37] to result from the maximum-likelihood formulation of receiver design. However, a receiver of this type is not easy to implement, and the receiver of [37] is not even the most general receiver structure for this problem, since it is based upon a set of discrete input samples, not upon the actual continuous-time waveform. In this paper, we are going to describe various receiver designs which, while not optimal, demonstrate very good performance when used to detect spread spectrum waveforms received in the presence of narrow-band interference, and which are all practical structures in the sense of being implementable with state-of-the-art technologies.

If, indeed, the interference is relatively narrowband compared with the bandwidth of the spread spectrum waveform, then the technique of interference cancellation by the use of notch filters often results in a large improvement in system performance, and the purpose of this paper is to illustrate several such spectral filtering techniques. In particular, the use of tapped delay line-type structures to implement notch filters is discussed below in a good deal

of depth. These notch-filters are used to further enhance the performance of a spread spectrum system over and above what the inherent processing gain of the system provides, and so, in this sense, they complement the spreading technique.

Consider the following: If, after spreading the spectrum of the underlying information over the maximum bandwidth available to the system, the resulting interference rejection capability is still not large enough to sufficiently attenuate any undesired signal, some additional means of interference removal must be used. With respect to the use of notch filters for this purpose, there appear to be two techniques that have received the most interest. The first technique, described in references such as [17], [20], [22], [18], uses a tapped delay line to implement either a one-sided prediction-error filter (Weiner filter [39]), or a two-sided filter. The basic rationale for the use of, say, the Weiner prediction filter for narrow-band interference suppression can be easily seen. The incoming waveform to the spread spectrum receiver consists of the desired spread spectrum signal (taken to be a binary phase-shift keyed (BPSK) direct sequence (DS) signal), thermal noise, and the narrow-band interference. Since both the DS signal and the thermal noise are wide-band processes, their future values cannot be readily predicted from their past values. On the other hand, the interference, being a narrow-band process, can indeed have its future values (and, in particular, its current value) predicted from past values. Hence, the current value, once predicted, can be subtracted from the incoming signal, leaving a waveform comprised primarily of the DS signal and the thermal noise. The same general philosophy holds for the two-sided transversal filter, except now the estimate of the present value of the interference is based upon both past and future values, and the improvement in system performance alluded to above is due to the use of both the past and the future to estimate the present.

The second technique is that of transform domain processing as described, for example, in [31]–[33]. In this technique, a tapped delay line, typically implemented with a surface acoustic wave (SAW) device, with a chirp impulse response built into the taps, is used as a real-time Fourier transformer. As described fully below, a notch filter is implemented by Fourier transforming the received waveform, using an on-off switch to perform the notching operation, and then inverse transforming.

In considering these techniques, both the similarities and the differences become evident. Both techniques can use tapped delay-line implementations, and both can be made adaptive. In the former scheme, the system can be made adaptive by using a tapped delay line with variable tap weights. These tap weights can be adapted, for example, by using the well-known least-mean-square (LMS) algorithm (see below). In the latter technique, it will be shown that an envelope detector in cascade with a threshold crossing indicator can be used to determine the location (in frequency) of the narrow-band interference and hence adjust the position of the notch (or notches) to suppress the interference.

Because both schemes use tapped delay-line implementations, both systems can be built with either SAW technology [30] or CCD [9] technology. Which technology should be used typically depends upon the required bandwidth, with SAW devices being the obvious choice for very

wide-band communication (e.g., bandwidths on the order of 100 MHz or more).

One general problem associated with the actual implementation of either of these two systems is that of dynamic range. Since, by definition, these systems are intended to operate in large interference environments, the range of input levels that SAW devices and CCDs can handle is crucial. For example, a typical dynamic range for a SAW device when used as a real-time Fourier transformer is about 40 dB. Yet if the SAW device is part of a system designed for antijam (A-J) protection, variations of input level could be 80 dB or more.

II. ESTIMATION-TYPE FILTERS

As we have noted, in a spread spectrum communication system employing a direct-sequence pseudonoise spreading signal, the effect of narrow-band interference on system performance is reduced due to the inherent processing gain of the system. However, when the processing gain is insufficient due to bandwidth restriction to allow satisfactory communication to take place, one technique which can at times improve the performance of the system is the method of interference rejection to be described in this section.

Fig. 1 shows the essential parts of a receiver using a suppression filter, and Figs. 2 and 3 show the two-sided and one-sided filter structures, respectively. The one-sided filter is often referred to as a prediction-error filter.

If we assume the spread spectrum signal samples taken at different taps are not correlated (see below), and if there
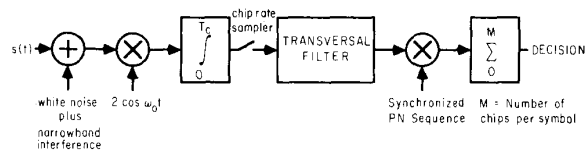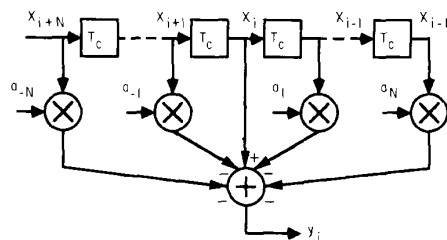

Fig. 1. Receiver block diagram.

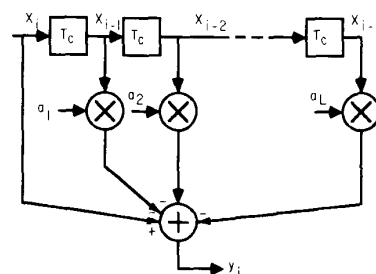**Fig. 2.** Two-sided transversal filter.

Fig. 3. Single-sided transversal filter.

is only white noise interference, the tap weights will be zero to maintain minimum output error power. If there is additional narrow-band interference, the tap weights will be adjusted to predict the input signal so that the resulting mean-squared error is minimized. The level of the interference is reduced at the expense of introducing some distortion on the desired signal.

There are many references available on this type of suppression filter, and they fall into several general categories. The first group of references emphasize the analytic enhancement in system performance achievable by the use of such filters as determined by the signal-to-noise ratio (SNR) improvement factor of the system. This improvement factor is typically defined as the ratio of the SNR with the suppression filter in the system to the SNR of the system operating without the rejection filter [17], [20], [22], [26], [27], [50], [24].

As is well known in digital communications, while SNR provides a good qualitative indication of system performance, it often does not provide a good quantitative description. To obtain the latter it is necessary to use average probability of error as the criterion-of-goodness, and both analytical [18], [19], [28] and experimental [44]–[47] investigations have been conducted.

A. Signal-to-Noise Ratio Improvement

To understand the operation of this type of suppression filter, consider the two-sided filter of Fig. 2. The received waveform consists of a binary phase-shift-keyed direct sequence spread spectrum waveform, a single tone interfering signal of known amplitude and frequency but with a random phase, and thermal noise. That is, the input to the receiver, $r(t)$, is given by

$$r(t) = s(t) + I(t) + n_w(t), \tag{1}$$

where

$$s(t) = Ac(t)\, d(t)\cos \omega_0 t \tag{2a}$$

$$I(t) = \alpha \cos\left[(\omega_0 + \Omega)t + \theta\right] \tag{2b}$$

and $n_w(t)$ is AWGN of two-sided spectral density $\eta_0/2$. In (2), A and α are constant amplitudes, θ is a random phase uniformly distributed in $[0, 2\pi]$, $d(t)$ is a random binary sequence of data symbols taking on values ± 1 with equal probability which last for T seconds, ω_0 is the carrier frequency of the transmitted signal, Ω is the frequency offset of the interference, and $c(t)$ is the spreading sequence taking on values ± 1 which last for T_c seconds, where $T_c \ll T$. The most common type of spreading sequence is a pseudonoise (PN) sequence [41], [42], [49], [54].

For simplicity, assume that we can coherently demodulate the received waveform with the reference $2\cos \omega_0 t$, as shown in Fig. 1. In reality, to accomplish this operation before despreading is not realistic [41], but there are straightforward techniques to circumvent this problem, and

in any event, the essence of the interference rejection mechanism is not dependent upon this assumption (see [46]). Hence, we assume that the sample on the central tap of the rejection filter shown in Fig. 2 at time iT_c is given by

$$x_i = d_i + V\cos(\Omega i T_c + \phi) + n_i \tag{3}$$

where, from Fig. 1 and (1) and (2), it is straightforward to show that

$$d_i = \pm A T_c \tag{4a}$$

$$V = 2\alpha\, \frac{\sin \dfrac{\Omega T_c}{2}}{\Omega} \tag{4b}$$

and

$$\phi = \theta - \frac{\Omega T_c}{2}. \tag{4c}$$

Also, for ease of notation, we let $AT_c = \sqrt{S}$, so that $d_i = \pm\sqrt{S}$, where the $\pm$ is determined by the combination of algebraic signs of the data symbol and the symbol of the spreading sequence (typically referred to as a "chip") at the current instant of time.

Let us now define two $2N$-dimensional vectors X_i and W as

$$X_i \triangleq [x_{i+N}, x_{i+N-1}, \cdots, x_{i+1}, x_{i-1}, \cdots, x_{i-N}]^t$$

and

$$W \triangleq [a_{-N}, a_{-N+1}, \cdots, a_{-1}, a_1, \cdots, a_N]^t$$

respectively, where t denotes transpose, X_i is the sample vector of the off-center taps at time iT_c, and W is the adjustable tap weight vector. Hence, the output sample of the filter is

$$y_i = x_i - W^t X_i. \tag{5}$$

Upon squaring (5), we obtain

$$y_i^2 = x_i^2 - 2x_i X_i^t W + W^t X_i X_i^t W \tag{6}$$

and thus, the expected value of y_i^2 (or the output power) is given by

$$E[y_i^2] = E[x_i^2] - 2E[x_i X_i^t]W + W^t E[X_i X_i^t]W$$

$$\triangleq E[x_i^2] - 2P^t W + W^t RW \tag{7}$$

where P and R are defined by (8) and (9), respectively, below.

Since the signal and the noise are independent, and assuming that the period of the PN sequence is sufficiently long so that the PN signal samples at different taps are approximately uncorrelated (see [41], [42], [49], [54] for the autocorrelation function of a PN sequence), then

$$P^t \triangleq E[x_i X_i^t]$$

$$= [J\cos N\Omega T_c, J\cos(N-1)\Omega T_c, \cdots,$$

$$J\cos \Omega T_c, J\cos \Omega T_c, \cdots, J\cos N\Omega T_c] \tag{8}$$

and

$$R \triangleq E[X_i X_i^t]$$

$$= \begin{bmatrix} S + J + \sigma_n^2 & J\cos \Omega T_c & \cdots & J\cos 2N\Omega T_c \\ J\cos \Omega T_c & S + J + \sigma_n^2 & \cdots & J\cos(2N-1)\Omega T_c \\ \cdots & \cdots & \cdots & \\ J\cos 2N\Omega T_c & J\cos(2N-1)\Omega T_c & \cdots & S + J + \sigma_n^2 \end{bmatrix} \tag{9}$$

where $J = V^2/2$ is the power of the interfering tone at the output of the integrator, σ_n^2 is the power due to the thermal noise, and S has been defined above. Equations (8) and (9) follow because, from (3), the autocorrelation function of x_i is given by

$$E[x_i x_{i+m}] = (S + \sigma_n^2)\delta(m) + J \cos m\Omega T_c$$

where $\delta(m)$ is the Kronecker delta function.

The tap weights $a_{-N}, \cdots, a_1, \cdots, a_N$ are adjusted to obtain minimum $E[y_i^2]$.[1] From (7), letting

$$\frac{\partial E[y_i^2]}{\partial a_k} = 0, \quad k = -N, \cdots, -1, 1, \cdots, N \quad (10)$$

we obtain

$$-2P + 2RW_{opt} = 0 \quad (11)$$

or

$$W_{opt} = R^{-1}P \quad (12)$$

where W_{opt} is the optimum tap weight vector. This, of course, is the well known Wiener–Hopf equation.

In [22], it is shown that the solution to (12) is

$$a_{k_{opt}} = 2\gamma \cos k\Omega t \quad (13)$$

where

$$\gamma = \frac{J}{2(S + \sigma_n^2) + J\left[2N - 1 + \dfrac{\sin (2N + 1)\Omega T_c}{\sin \Omega T_c}\right]}. \quad (14)$$

It is also shown in [22] that the minimum output noise power is given by

$$E[e^2]_{min} = \frac{J}{1 + \dfrac{J}{2(S + \sigma_n^2)}\left[2N - 1 + \dfrac{\sin (2N + 1)\Omega T_c}{\sin \Omega T_c}\right]} + \sigma_n^2.$$

$$(15)$$

If the signal-to-noise ratio improvement factor G is defined as the ratio of the output SNR to the input SNR, then G_2, the improvement factor for the transversal filter of Fig. 2, is given by

$$G_2 = \frac{(S/N)_{out}}{(S/N)_{in}}$$

$$= \frac{J + \sigma_n^2}{\dfrac{J}{1 + \dfrac{J}{2(S + \sigma_n^2)}\left[2N - 1 + \dfrac{\sin (2N + 1)\Omega T_c}{\sin \Omega T_c}\right]} + \sigma_n^2}.$$

$$(16)$$

Note that this ratio of SNR's is consistent with the definition of the SNR improvement factor given at the beginning of this section. In particular, with no suppression filter, the SNR is

$$SNR_{nf} = \frac{S}{J + \sigma_n^2}$$

while with the suppression filter in place, the SNR is given by

$$SNR_f = \frac{S}{E(e^2)_{min}}$$

where $E(e^2)_{min}$ is given by (15). Taking the ratio of SNR_{nf} to SNR_f then yields (16). Notice also that, for this problem, minimizing the output noise power corresponds to maximizing the SNR.

In the extreme case, if $\sigma_n^2 = 0$

$$G_2 = 1 + \frac{J}{2S}\left[2N - 1 + \frac{\sin (2N + 1)\Omega T_c}{\sin \Omega T_c}\right]. \quad (17)$$

From (17), we see that G_2 increases either as the number of taps increases or as the input interference-to-signal power ratio J/S increases. Fig. 4 shows an example where $2N = 10$, $\sigma_n^2 = 0$, and $J/S = 100$. Also shown on Fig. 4 are comparable
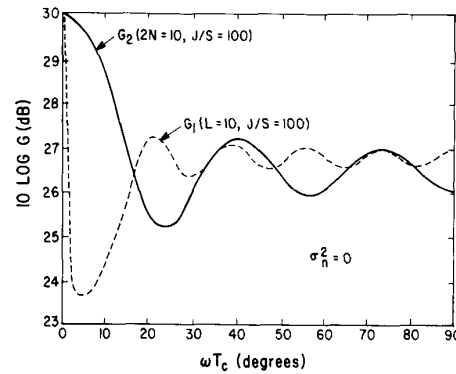

Fig. 4. Output signal-to-noise ratio improvement versus ωT.

results for G_1, the improvement factor for the prediction-error filter of Fig. 3. Analytically, this latter expression is given by

$$G_1 = \frac{J + \sigma_n^2}{2(S + \sigma_n^2)\left[\left(L + \dfrac{2(S + \sigma_n^2)}{J}\right) - \dfrac{\sin L\Omega T}{\sin \Omega T}\cos (L + 1)\Omega T\right]\Big/\left[\left(L + \dfrac{2(S + \sigma_n^2)}{J}\right)^2 - \dfrac{\sin^2 L\Omega T}{\sin^2 \Omega T}\right] + \sigma_n^2}.$$

Finally, if one computes the transfer function of the two-sided filter, it can be shown that [22]

$$H(w) = 1 - \frac{J\left[\left(\sin \dfrac{(2N + 1)(\omega + \Omega)T_c}{2}\Big/\sin \dfrac{(\omega + \Omega)T_c}{2}\right) + \left(\sin \dfrac{(2N + 1)(\omega - \Omega)T_c}{2}\Big/\sin \dfrac{(\omega - \Omega)T_c}{2}\right) - 2\right]}{2(S + \sigma_n^2) + J\left[2N - 1 + \dfrac{\sin (2N + 1)\Omega T_c}{\sin \Omega T_c}\right]}.$$

[1] Note that since y_i is the difference between x_i and the weighted sum of the remaining x_{i+j}, $|j| = 1, 2, \cdots, N$, minimizing $E\{y_i^2\}$ corresponds to minimizing the mean-square error between x_i and its estimate.

Fig. 5 shows an example of a transfer function where $N = 5$, $\sigma_n^2 = 0$, $J/S = 100$, and $\Omega T_c = \pi/3$. It can be seen that $H(\omega)$ behaves as a notch filter.
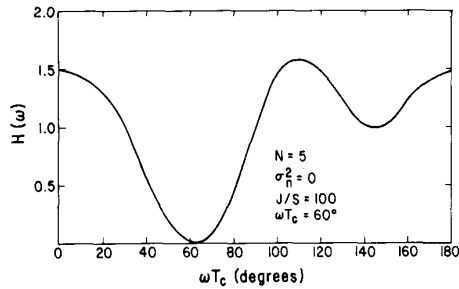
Fig. 5. Frequency response of the transversal filter.

Fig. 8. Tone jammer performance with varying amplitude.

The above analysis is especially straightforward because it corresponds to SNR at the output of the suppression filter rather than SNR at the output of the final detection filter. For analyses that incorporate the final despreading and low-pass filtering, the reader is referred to [17], [20], [26], [27]. Also, for analyses dealing with multiple narrow-band interferers rather than just a single source, references [20], [51], [24] are appropriate. Finally, while the results presented here are for BPSK systems, analogous results exist for quadrature phase-shift keyed (QPSK) receivers [23], [25]. Although the suppression filter for a QPSK signal is more complex than it is for a BPSK waveform, the results are qualitatively very similar.

B. Average Probability of Error

Let us now consider the block diagram of Fig. 6. This system is analyzed in depth in [18], from which the following results are taken. The expression for probability of error is quite lengthy and is not presented here. However, typical performance results are shown in Figs. 7–10. In Fig. 7, prob-
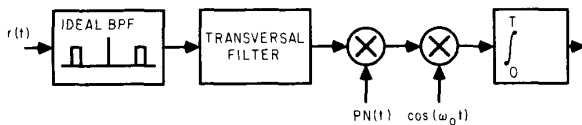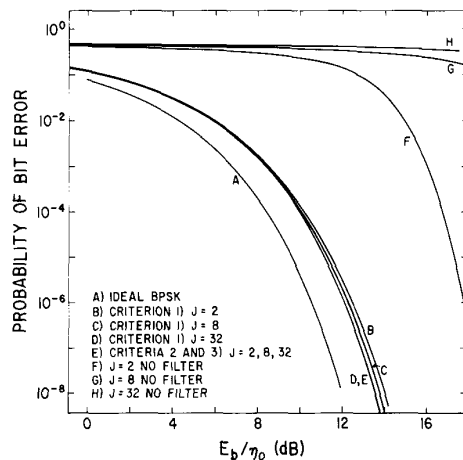

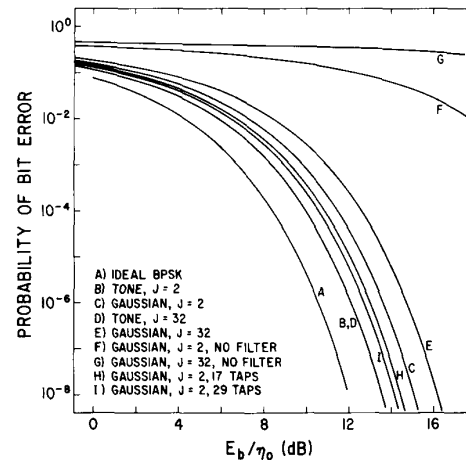
Fig. 6. Receiver block diagram.

Fig. 9. Comparison between tone and narrow-band gaussian interference. Bandwidth of gaussian interference equals 10 percent of front-end bandwidth.

Fig. 7. Tone jammer performance for a 4-tap filter under Criteria 1, 2, and 3.
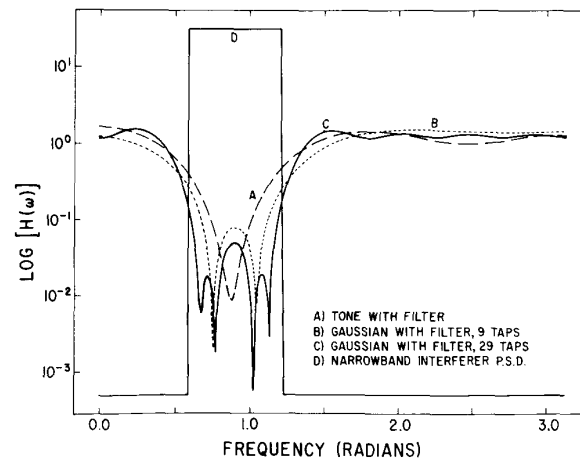

Fig. 10. Frequency responses of suppression filters.

ability of error curves are presented for a simple DS system employing a processing gain of seven (i.e., there are seven chips/bit) when a tone interferer is located at a frequency which is offset from the carrier frequency of the DS waveform by an amount equal to the symbol rate (i.e., Ω in (2b) equals $2\pi/T$).

There are three different design criteria used to set the tap weights for the system of Fig. 6. Criterion 1 corresponds to whitening (i.e., making the output samples uncorrelated) the entire received signal. It can be shown that this is equivalent to the intuitive procedure described at the beginning of this section, namely, predicting the current value of the received waveform and subtracting that predicted value from the received value [34]. Criterion 2 corresponds to whitening the noise and interference only (see the discussion on decision feedback filters near the end of this section), and the last criterion, Criterion 3, corresponds to designing the filter so that an infinitely deep notch is placed at the frequency location of the interfering tone.

In Fig. 7, the probability of error is plotted versus the ratio of energy-per-bit-to-noise spectral density, E_b/η_0, for interference powers of 2, 8, and 32 for each of the three filter design criteria. The noise spectral density η_0 is fixed at 1/8, so that when E_b equals 1/2, the resulting E_b/η_0 is 6 dB. Note that under Criterion 1, performance improves as the interference power increases from 2 to 32 (see below for the explanation). In Fig. 8, E_b/η_0 is fixed at 10 dB and the sensitivity of system performance to the amplitude of the interference is illustrated. Note that the performance under Criterion 3 is invariant to changes in interference amplitude since the tone is always completely rejected by the infinitely deep notch filter.

From Fig. 8, it is seen that the Criterion 2 leads to the best system performance. It appears that under Criterion 3, the notch deepens too rapidly (its depth is infinite for any finite J), while for Criterion 1, the notch does not deepen rapidly enough. Indeed, the seemingly strange behavior of the receiver designed using the Criterion 1 suppression filter referred to above, namely giving better performance for a higher level of interference, is due to the suboptimal balance achieved by the filter in terms of minimizing the degradation to the DS signal while maximizing the interference rejection. That is, over a fairly wide range of input signal levels, the receiver designed by this criterion is too conservative in the sense of not forcing the notch to be deep enough, and hence resulting in insufficient interference suppression. Note, however, that for a large enough interferer, the performance of the system designed under any one of the three criteria converges to the same result.

It is seen that when the interference is a pure tone, increasing the tone power has no effect on system performance when the notch is infinite. However, when the interference has a finite spectral width, it cannot be completely rejected by a suppression filter with a finite number of taps, since only a finite number of zeros can be placed in the frequency band spanned by the interference. This is illustrated in Fig. 9, where the interfering tone of (2b) has been replaced with an interferer modeled as a stationary, zero-mean, narrow-band gaussian random process. The remaining parameters of the system are fixed at those used for the tone interference, and the bandwidth of the narow-band process ω_j is set at 10 percent of the receiver front-end bandwidth. It is easily seen that the suppression filter is less

effective against a source of interference with a finite (i.e., nonzero) spectrum, than it is against a tone of equivalent power. It is also seen that performance against the narrow-band gaussian process can be improved by increasing the number of taps in the suppression filter. Finally, in Fig. 10, the magnitudes of the frequency responses of the suppression filters designed under Criterion 2 are plotted for both narrow-band gaussian and tone interference. It is seen that the change in the filter notch for the gaussian interferer as the number of taps is increased from 9 to 29 becomes quite noticeable.

An alternate block diagram for a system of this type is shown in Fig. 11. This system is amenable to implemen-
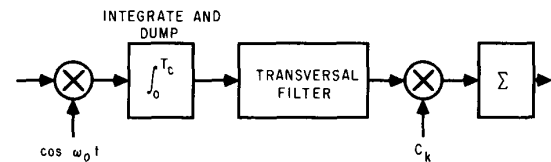

Fig. 11. Suppression filter suitable for CCD or DSP implementation.

tation with the type of processing inherent with either charge-coupled devices or digital signal processing, and in [18], results similar to those shown in Figs. 7-10 for the system of Fig. 6 are presented for the system of Fig. 11.

Note that all results presented up to this point have assumed precise statistical knowledge of the interference. In reality, such information is rarely available, hence one must envision implementing an adaptive version of the rejection filter. There are a variety of adaptive algorithms that can be used, as well as a variety of receiver structures [20], [19], [14], [21], [50].

For the results presented here, the adaptive version of the system uses the Widrow–Hoff LMS algorithm [52], [53] to update the tap weights. This algorithm is probably the best known of a class of algorithms designed to implement an iterative solution to the Wiener–Hopf equation without making use of any a priori statistical information about the received signal. The LMS algorithm can be expressed as

$$W^{(k+1)} = W^{(k)} + \mu y^{(k)} X^{(k)}$$

where $W^{(k)}$ is the vector of tap weights, $X^{(k)}$ is the vector of waveform samples on the taps, $y^{(k)}$ is the difference between the waveform sample on the reference tap (denoted $x_0^{(k)}$) and the estimate of that same sample (i.e., $y^{(k)}$ is given by

$$y^{(k)} = x_0^{(k)} - W^{(k)t}X^{(k)}),$$

all at the kth adaptation, and μ is a parameter which determines the rate of convergence of the algorithm. In other words, the parameters $W^{(k)}$, $X^{(k)}$ and $y^{(k)}$ are the same as those defined in (3), (2), and (5), respectively, except now the notation has been slightly changed to indicate the explicit dependence on the iteration value k. It is interesting to note that in most applications of the LMS algorithm [52], an external reference waveform is needed in order to correctly adjust the tap weights. However, in this particular application, the signal on the reference tap (e.g., the center tap of a two-sided symmetrical tapped delay line) serves the role of the external reference.

The analysis of the performance of an adaptive receiver

employing the LMS algorithm analysis is very difficult. An approximate analysis is presented in [19], and typical results are shown in Fig. 12. Curve *B* is the exact probability of error
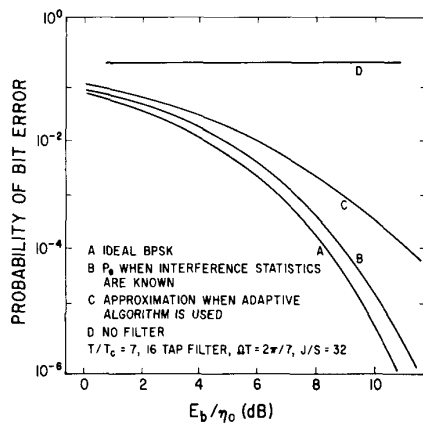

Fig. 12. Performance of adaptive receiver.

of the system when the statistics of the interference are precisely known (and hence the LMS algorithm is not needed), while curve *C* corresponds to the approximate results derived in [19]. That is, they correspond to a receiver using the LMS algorithm to adjust the tap weights. Upon comparing curves *B* and *C* of that figure, the degradation incurred by the lack of knowledge of the statistics of the interference is easily seen.

In order to explore this effect further, the system shown in Fig. 11 was implemented using charge-coupled devices, and, independently, using digital logic. The former system is described in [44], and the latter system is described in [45]. In what follows, a brief overview of the digital system is presented.

As noted in [45], direct implementation of the LMS algorithm requires two multipliers per filter tap, one to perform the update operation and a second to do the actual signal sample weighting. A block diagram showing a conventional implementation of the LMS algorithm is shown in Fig. 13.
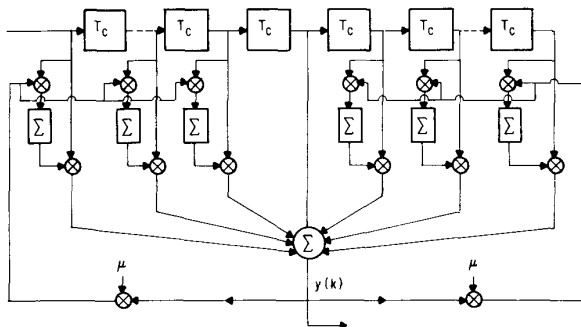

Fig. 13. Conventional implementation of LMS algorithm for a two-sided filter.

However, it is also possible to implement the algorithm using a so-called burst processing technique [44], [45], which allows the construction of a filter of arbitrary order using only two multipliers. However, the price for obtaining the

lower multiplier count while still updating all weights each sample period is a loss of bandwidth.

To illustrate this technique, a test configuration was set up and used to obtain probability of error data for the system. A 7-chip PN sequence is modulated by random data and added to a tone interferer and white gaussian noise. The composite signal is then adaptively filtered and correlated. A decision based on the correlator output is compared to the actual data sent and the number of errors that are made is counted. Fig. 14 shows a series of curves obtained using this test arrangement. Curve *A* is the the-
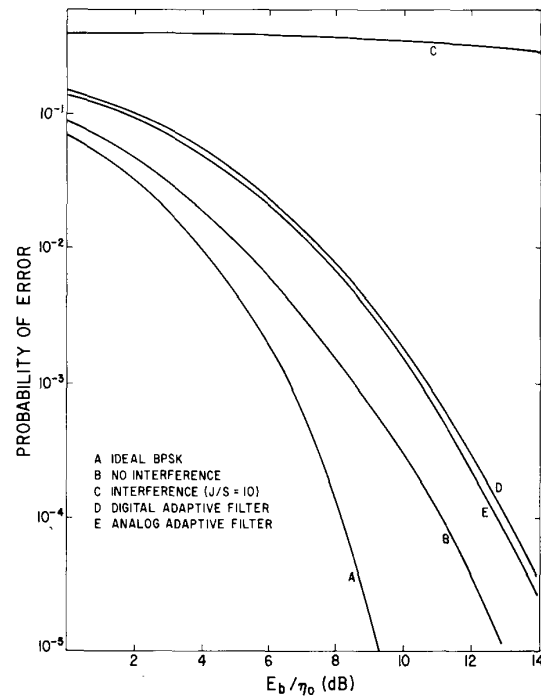

Fig. 14. Performance of both digital and CCD versions of adaptive filter.

oretical BPSK result while curve *B* is the system performance in the absence of both the interference and the adaptive filter. The degradation in performance from that of curve *A* is due to implementation losses. Curve *C* shows the effect of a tone interferer with J/S = 10 dB, again in the absence of the suppression filter. As expected, this results in an essentially useless system. Curve *D* shows the system performance with a 16-tap adaptive filter in the receiver. The interference suppression causes a significant improvement in the probability of error performance, although it does not completely remove the interference. The performance of the analog system of [44] for an interferer with J/S = 10 is given by curve *E*. The interference frequency for this result, as well as for the digital system, is $f_c/7$, where f_c is the chip rate (i.e., $f_c = 1/T_c$).

The curves of Fig. 14 demonstrate that the adaptive filter is providing a significant improvement in performance. As shown by curves *D* and *E* of Fig. 14, the results obtained with the digital system are nearly identical to those found using the analog version, although the sources of degradation differ for the two receivers. For the digital system, quan-

tization noise was the limiting factor, whereas for the analog system, charge transfer inefficiency [9] limited the overall receiver performance.

Up to this point, the transversal filter structure has been emphasized. However, other suppression filter structures do exist, and a couple of these are discussed below. Similarly, while the LMS algorithm has been discussed here as a means of making the system adaptive, there are other algorithms that are available for the same purpose, and which can, in addition, overcome certain drawbacks in the LMS algorithm. In particular, it is well known [53] that the convergence rate of the LMS algorithm is relatively slow, it being a function of the ratio of the maximum and minimum eigenvalues of the autocorrelation matrix R of (9). A good discussion of this can be found in [52]. Because of this drawback to the LMS algorithm, other structures have been investigated and one of the most popular is the lattice filter [1], [42]. A typical lattice structure is shown in Fig. 15. The
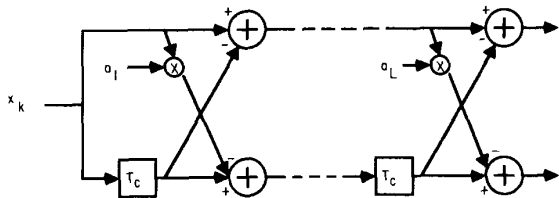

Fig. 15. Lattice filter.

layout of this filter is somewhat different from that of the transversal filter, and it is known that an adaptive version of this filter can result in much faster convergence than can the LMS algorithm, because each section of the lattice can be shown to converge individually, independent of the remaining sections (i.e., the various stages of the lattice are decoupled from one another).

In both [15] and [47], lattice filters used for narrow-band interference suppression are described. Simulation results for a two-stage lattice are described in [15], and experimental results for both three- and ten-stage lattice filters are presented in [47]. In all cases, significant improvement in performance over that of a DS system operating in the absence of a suppression filter is shown to be possible.

Another alternative to a transversal filter is a decision feedback (DF) filter [42], [21], [14], [23], [25]. One version of such a filter is shown in Fig. 16 and analyzed in [50]. The
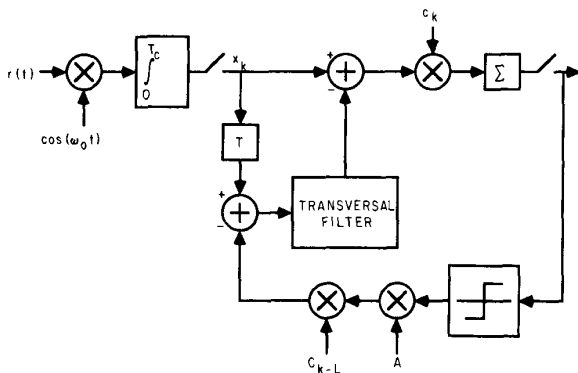

Fig. 16. Decision feedback receiver.

rationale for this scheme is that if one could whiten just the noise and interference (i.e., without the desired signal being present), the performance of the system might improve (in fact, this idea was presented briefly at the beginning of this section as the second of the three criteria described for the filter design).

The principle behind the operation of a DF filter is quite simple. Since the received waveform consists of the desired signal plus noise and interference, to whiten just the noise and interference, some means of removing the desired signal is necessary. However, since the output of the receiver is an estimate of the data symbol that has been transmitted, that estimate can be used to generate a replica of the transmitted waveform which, in turn, can be subtracted from the received signal. If the decision the receiver makes on the current data symbol is correct, the subtraction referred to above results in just noise plus interference, and hence, the output of this subtractor can be used as the input to a filter designed to whiten its input.

Of course, if the decision on the data symbol is incorrect, the input to the whitening filter consists not only of noise plus interference, but also twice the desired signal component. Hence, the possibility exists for error propagation. If one considers first the idealized case of perfect (i.e., error-free) decision feedback, results such as those obtained in [50] and presented in Fig. 17 are available. The interference
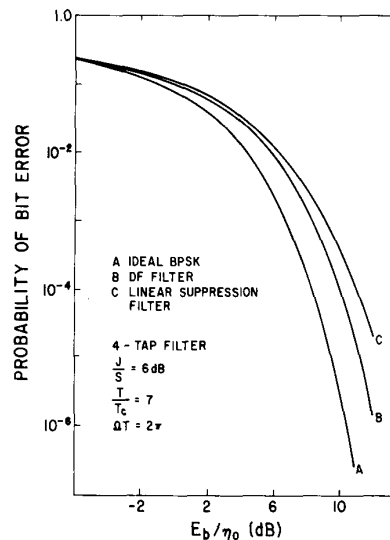

Fig. 17. Comparison of linear filter and DF filter under perfect DF conditions.

is a single tone, and the results correspond to a four tap filter, $T/T_c = 7$, $J/S = 6$ dB and $\Omega T = 2\pi$. Upon comparing the DF performance of curve B with that of curve C, which corresponds to a linear suppression filter of the same size, the potential improvement in using the DF structure is evident.

This potential improvement could, of course, be negated by the effect of decision feedback errors. Interestingly however, for this system such an effect appears to be negligible. Specifically, simulation results generated in [50] and illustrated in Fig. 18 compare the performance of the system operating under the assumption of perfect decision feed-
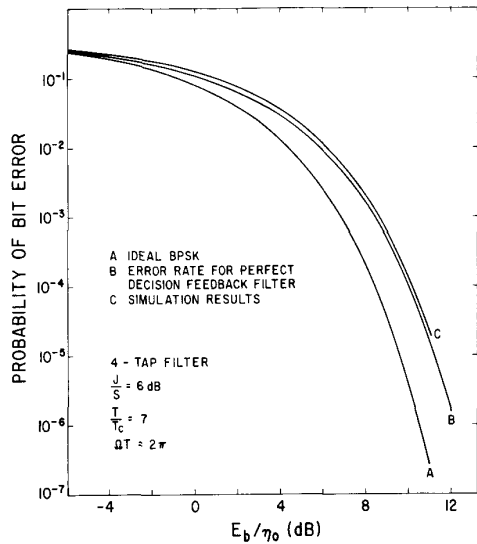
Fig. 18. BER for tone jammer for DF filter.

back to that of the system operating in the presence of error propagation, and, as can be seen, show the effect of error propagation to be minimal.

As a final point of interest, since these techniques are most appropriate for narrow-band interference suppression, a natural question that arises is "What is the definition of 'narrowband'?" While no precise answer to that question appears to be available, some perspective on the answer can be obtained by considering some of the results presented in [28]. In [28], the "worst-case" spectral density of a gaussian interferer was found. The interferer's spectral content was nonzero over only a prespecified fraction of the spread bandwidth, and the spectrum of the interference was optimized to maximize the mean-square error at the output of an infinitely-long prediction filter. The resulting interferer was then used in a system with a finite length filter, and the average probability of error of the receiver was derived.

The resulting performance can be seen in Figs. 19 and 20, corresponding to $\lambda = 0.1$ and 0.5, respectively, where λ represents the percent of the spread bandwidth occupied by the interference. In both cases, the center frequency of the interference coincides with the carrier frequency of the

Fig. 19. P_e versus E/η_0 for interference centered about carrier frequency.

Fig. 20. P_e versus E_b/η_0 for interference centered about carrier frequency.

transmitted signal. It is seen that when $\lambda = 0.1$, the rejection filter is very effective, yet when $\lambda = 0.5$, the filter is almost worthless. Figs. 21 and 22 show the magnitudes of the transfer functions of the filters corresponding to $\lambda = 0.1$ and 0.5, respectively. Both the filters are notch-filters, but the notch corresponding to $\lambda = 0.5$ is so wide that it results in significant distortion to the desired signal.

Fig. 21. Filter amplitude response.

Fig. 22. Filter amplitude response.

III. Transform Domain Processing

A receiver which performs the notch filtering operation in a completely different manner from the systems described in Section II is the so-called transform domain processing system [38], [4], [36], [7], [8]. The basi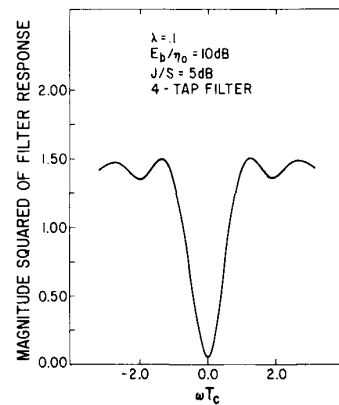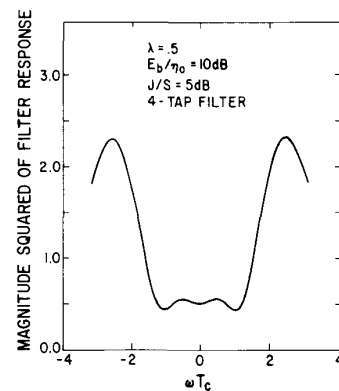c building block of such a system is a device which performs a real-time Fourier transform. For spread spectrum applications, this device is typically a SAW device. In what follows in this section, we briefly review the technique of real-time Fourier transformation, and then describe and analyze the transform domain processing system. Most of the material in this section is taken from [29], [31], [32], [48].

The receiver to be analyzed is that described in [31] and shown in Fig. 23. The input consists of the sum of the trans-
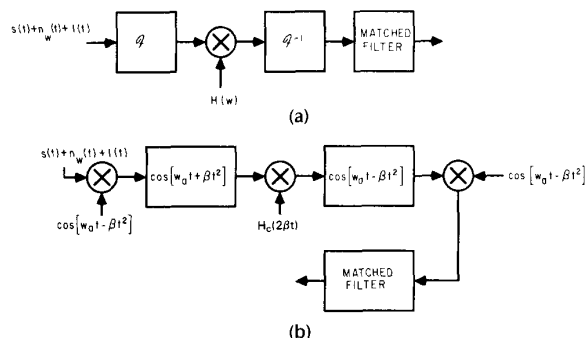

Fig. 23. Receiver block diagram for transform domain processing system. (a) Functional operations. (b) Actual implementation.

mitted signal $\pm s(t)$, AWGN $n_w(t)$, and the interference $I(t)$. The Fourier transform of the input is taken, the transform is multiplied by the transfer function of some appropriate filter $H_c(w)$, the inverse transform of the product is taken, and the resulting waveform is put through a detection filter matched to $s(t)$.

Intuitively, if one considers the spectra of the signal and interference components of the input $r(t)$, it can be seen why the receiver shown in Fig. 23 can be expected to provide interference suppression. On the one hand, we have a low level, broad-band DS spectrum; on the other hand, we have added to it a high level but narrow-band interference waveform. Since the output of the Fourier transformer shown in Fig. 23 is a waveform evolving in real-time which looks qualitatively like the one shown in Fig. 24(a), multiplying that output by the waveform shown in Fig. 24(b) should suppress a significant amount of interference power while only slightly reducing the power of the desired signal. This heuristic explanation will be shown to indeed be accurate. Note that while the abscissas in Fig. 24(a) and (b) are labeled ω, the variable ω is actually a linear function of time.

Let us now consider analyzing the performance of this receiver. Since the system is linear, the three components of the input can be treated separately. Denoting any one of them by $f(t)$, assumed nonzero for $t \in [0, T]$, the signal at the output of the first SAW device is given by

$$f_1(t) = \int_0^T f(\tau) \cos (w_a \tau - \beta \tau^2) \cos (\omega_a(t - \tau) + \beta(t - \tau)^2) \, d\tau$$
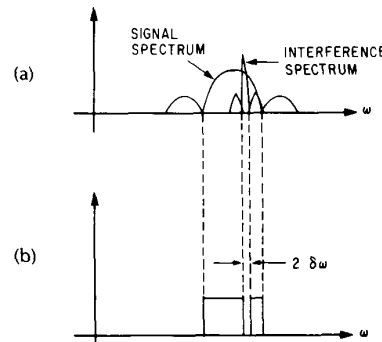
$$(18)$$

Fig. 24. Notch filter.

an expression which is valid for $t \in [T, T_1]$, where T_1 is the length of the SAW device in seconds (see below for the explanation).

Simplifying, this yields

$$f_1(t) = (1/2) \cos (\omega_a t + \beta t^2) \int_0^T f(\tau) \cos 2\beta t\tau \, d\tau$$

$$+ (1/2) \sin (\omega_a t + \beta t^2) \int_0^T f(\tau) \sin 2\beta t\tau \, d\tau$$

$$+ 1/2 \int_0^T f(\tau) \cos (2\omega_a \tau - 2\beta \tau^2$$

$$+ 2\beta t\tau - w_a t - \beta t^2) \, d\tau \qquad (19)$$

$$\simeq (1/2) F_R(2\beta t) \cos (\omega_a t + \beta t^2) - (1/2) F_I(2\beta t)$$

$$\cdot \sin (\omega_a t + \beta t^2) \qquad (20)$$

where $F_R(\omega)$ and $F_I(\omega)$ are the real and imaginary parts, respectively, of the transform of $f(t)$, and the approximation used in going from (19) to (20) is to ignore the third term of (19), which is a double frequency term. Alternately, if it is desired to exactly cancel the third term, one can implement a system described in [31]. Note that this latter system requires twice as much equipment and, as a practical matter, is usually not needed, since the double frequency term is almost always filtered out to a sufficient degree by the receiver of Fig. 23.

The important thing to observe about (20) is that the real and imaginary components of the transform of $f(t)$ are modulating quadrature carriers, meaning both components have been individually recovered and thus the Fourier transform itself has been recovered (over a finite interval in the frequency domain). Another point worth emphasizing is that (20) only yields the correct values of $F_R(2\beta t)$ and $F_I(2\beta t)$ when $f(t)$ is indeed nonzero only for $t \in [0, T]$. Such would be the case, say, for one pulse in a digital pulse stream where the duration of each pulse is T seconds, and where $T < T_1$. However, it would not be the case for a waveform which may be greater than T seconds in duration, such as the noise. For such waveforms, (20) yields the Fourier transform of the time-truncated signal, not of the signal itself.

Note that (20) does not yield the Fourier transform of $f(t)$ for all $2\beta t$ (i.e., for all ω). Rather, (20) yields $F(\omega)$ only during that interval of time when $f(t)$ is fully contained in the tapped delay line. Since the delay line is T_1 seconds long and since the duration of $f(t)$ is T seconds, the frequency range over which (20) yields a true Fourier transform is $w \in [2\beta T, 2\beta T_1]$.

Having transformed $f(t)$, it is now desired to filter it with a filter whose transfer function is $H(w)$. In Fig. 23, it can be seen that the output of the first chirp filter is multiplied by $H_c(2\beta t)$. This function is related to the desired transfer function $H(w) = H_R(w) + jH_I(w)$ by

$$H_c(2\beta t) = 4H_R(2\beta t) \cos 2\beta t T_1 + 4H_I(2\beta t) \sin 2\beta t T_1. \quad (21)$$

The terms $\cos 2\beta t T_1$ and $\sin 2\beta t T_1$ shift the region the input signal is located in from $[0, T]$ to $[T, T_1 + T]$. This is necessary because the inverse transform filter can be shown to yield an accurate inverse transform only in the range $t \in [T_1, T_1 + T]$. This follows from the same argument used to define the region that the forward transform is valid in, namely, that the inverse transform is only valid when the entire forward transform is contained in the tapped delay line used to perform the inverse. In the remainder of this section, it is assumed that the filter is purely real, so that $H_I(w) \equiv 0$.

Proceeding further with the analysis, it is shown in [31] that the component of the final output of the system due to $f(t)$, when sampled at $t = T_1 + T$, is given by

$$f_0(T_1 + T) = \int_0^T f(t)[h_R(t) * s(t)] \, dt \quad (22)$$

where $h_R(t)$ is the inverse Fourier transform of $H_R(w)$ and $*$ denotes convolution. Finally, it is possible to implement an adaptive version of this system as described in [48] and illustrated in Fig. 25. Its operation can be seen as follows: The
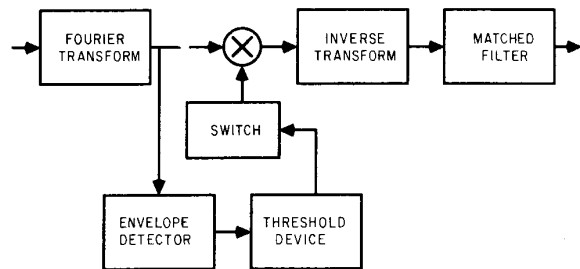

Fig. 25. Block diagram of adaptive transform domain processing receiver.

lower branch envelope detects the Fourier transformed input, and the output of the envelope detector is fed into a switch controlled by a threshold device. The upper branch passes the Fourier transformed input directly to the multiplier. The switch in the lower branch is set so that any time the output of the envelope detector exceeds a predetermined level, the output of the switch is forced to zero (and hence the lower input to the multiplier is also zero). In this manner, the adaptive notch switch is implemented.

To determine the amount of improvement in average probability of error that a technique such as transform domain processing can provide, results derived in [32] are used. The received waveform to the system shown in Fig. 23 is again given by (1) and the actual expressions needed to determine the average probability of error are given in [31] and are not repeated here. Rather, results obtained from evaluating those expressions are presented below, along with system comparisons and perspectives. Further results can be found in [32].
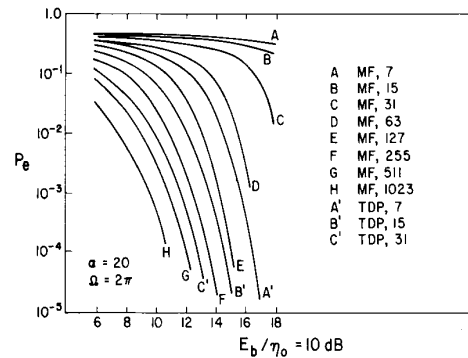

Fig. 26. Comparison of performance of transform domain processing receiver and conventional DS receiver.

Fig. 26 shows curves of average probability of error for both the transform domain processing system and a conventional system. By a "conventional system," we mean a DS receiver that is not employing the suppression filter. The curves are labeled with a number (e.g., 31) indicating the processing gain of the system (in all cases a full period of the spreading sequence is superimposed upon each data symbol), as well as either the abbreviation of MF, which stands for "matched filter," or the abbreviation TDP, which stands for "transform domain processing."

This figure indicates the processing gain needed in the conventional system (i.e., the MF system) to yield comparable performance to that of the transform domain processing system for a given interference level α. For example, from Fig. 26, corresponding to $\alpha = 20$ and $\Omega T = 2\pi$, a conventional DS spread spectrum system would have to operate with a processing gain somewhere between 255 and 511 in order to yield the same probability of error performance that the transform domain processing system yields with a processing gain of 31. Hence the improvement is a factor of about 10 dB.

As another perspective on the performance of such a system, an experimental version was implemented and various results are documented in [43] and [10]. In Fig. 27, some of these experimental results are reproduced. The spread spectrum code used for the experiment is a 63 chip PN
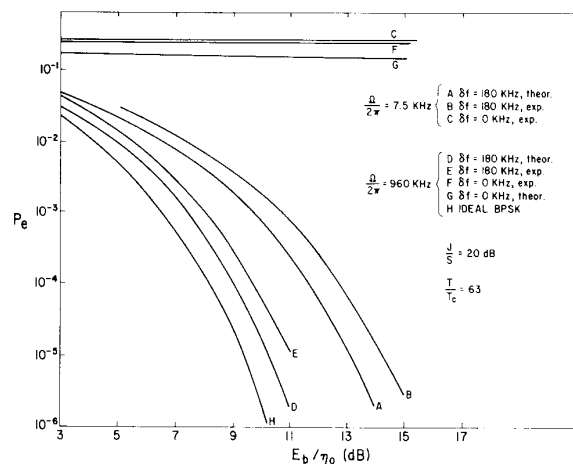

Fig. 27. Comparison of measured and theoretical results.

sequence with a chip rate of 1.875 MHz. The Fourier transform of this signal is obtained at the output of a real-time Fourier transformer which uses chirp devices with center frequencies of 15 MHz, bandwidths of 7 MHz, interaction times of 117 μs and chirp rates of 3×10^{10} Hz/s. Thus, in the frequency domain, 1 μs corresponds to 60 kHz and the main lobe of the transform of the desired signal has a width of 3.75 MHz.

Fig. 27 presents curves of probability of error versus energy-per-bit to noise spectral density ratio for the case of single tone interference. The curves are parameterized by the offset frequency Ω, and by whether-or-not the notch is employed. When the notch is indeed used, the notch width is fixed at 180 kHz. For the frequency offset, either 7.5 or 960 kHz is used. Theoretical curves are also presented in the same figure and the agreement is within a fraction of a decibel. To achieve adequate phase averaging, the single tone interferer is phase modulated with a phase excursion of $\pm \pi$ radians at 100 Hz. The signal power-to-interference power ratio is -20 dB for all the measurements shown.

Another consideration in the overall system design concerns the shape of the window used to "view" the received waveform. Rectangular windows were the ones used most often in the experiments, but it is well known that rectangular windows produce large sidelobes which can be reduced by proper weighting functions; however, these weighting functions distort the input signal itself.

In [10], an initial attempt was made to resolve this question, with typical results shown in Fig. 28. There are two curves shown on this figure, one corresponding to an unweighted system (i.e., a rectangular window) and the other corresponding to the use of a raised cosine window function. It is seen from Fig. 28 that at large values of J/S, the use of weighting provides the potential for a significant enhancement of system performance.
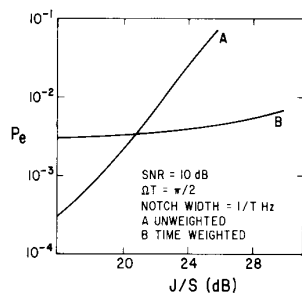

Fig. 28. Probability of error versus the interference power-to-signal power ratio.

It should be cautioned, however, that the above results were obtained under the assumption of perfect bit synchronization. Therefore, aside from the need to examine the effect of various other window shapes, it is necessary to investigate whether or not any weighting functions (other than the rectangular one) can be successfully used before synchronization has taken place. In addition, the overall sensitivity of a weighted system to timing errors must be determined.

The above results indicate the degree to which the technique of transform domain processing can reject either a

constant tone or a slowly varying tone. When the interference has a larger spectral width, the technique can still be used, and, as an example, the results presented in [33] correspond to the interference being a colored gaussian random process. For this situation, the multiplying transfer function is just the inverse of the power spectral density of the noise and interference.

IV. DETECTION OF SPREAD SIGNALS

In the previous two sections, the use of interference suppression techniques was discussed from the point of view of enhancing the performance of a spread spectrum receiver for which the intended signal is embedded in interference. That is, the receiver in question was the receiver to which the message was originally transmitted.

Consider now the opposite situation, namely one whereby the receiver of interest is not the intended receiver, but one which nevertheless is attempting to determine the presence or absence of the spread spectrum waveform. The use of a spread signal by a transmitter to "hide" its waveform from unintended receivers is another well-known application of spread spectrum techniques and is referred to as low probability of intercept, or LPI for short. In turn, a receiver whose goal is to learn whether or not such a signal is indeed being transmitted is often referred to as an intercept receiver. Reference [49] provides an introductory treatment of intercept receivers.

While there are many types of intercept receivers, only the most classical one is discussed here. That one is called a total power radiometer, and is shown in Fig. 29. It consists

Fig. 29. Radiometer.

of a bandpass filter, a square-law device and an integrator. Essentially, it looks for energy at dc by observing the output voltage of the integrator. If the voltage exceeds a predetermined threshold, signal-plus-noise is declared; if the voltage falls below the threshold, noise only is declared.

Suppose, however, that in addition to signal and noise, interference is also present at the input to the radiometer. This interference is not necessarily intentional interference, but could just be a conventional narrow-band waveform (i.e., not another spread spectrum signal) that happens to be present somewhere in the same frequency band as the signal the intercept receiver is attempting to detect. Then, upon squaring the composite received waveform, energy from each of the components is generated and contributes to the output voltage of the integrator. When signal is indeed present, the presence of the interference might actually aid in the detection of the signal since the interference is usually just adding to the total energy of the received waveform. However, when signal is absent, the radiometer might be deceived into believing the signal is actually present, because the presence of the interference is going to make it more likely that the integrator output voltage exceeds the threshold. In other words, the radiometer, being a device that bases its decision on the total received energy, cannot distinguish between energy due

to signal, energy due to noise, and energy due to interference.

Hence, the main effect of the interference is to increase the probability of false alarm. To combat this effect, an interference suppression filter can be used to reject the interference before the composite received waveform is squared, and initial results of using TDP to accomplish this goal are described in [11]-[13]. Fig. 30 shows a block diagram of the system, and Table 1 shows some measured results of probability of detection (P_d) and probability of false alarm (P_{fa}) taken from [12]. When the results are referred to as cor-
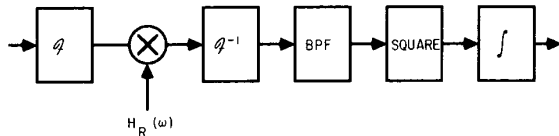

Fig. 30. Radiometer with interference suppression.

Table 1 Probability of Detection Versus False Alarm for Weighted and Un-Weighted Signal, with Excision Filter On and Off

Excision On				Excision Off	
Unweighted Signal		Weighted Signal		Weighted or Unweighted Signal	
P_{fa}	P_d	P_{fa}	P_d	P_{fa}	P_d
0.0025	0.59	0.0024	0.72	0.91	0.91
0.0042	0.73	0.0046	0.86	0.97	0.98
0.02	0.85	0.0075	0.9	0.98	0.98
		0.0094	0.92		

responding to a "weighted signal," it simply means that the input signal is multiplied by a nonrectangular window function prior to Fourier transformation. For the data presented in Table 1, the weighting corresponds to a four-term Blackman-Harris window. Also, the ratio of interference power-to-signal power is 28 dB, while the ratio of signal power-to-thermal noise power is 0 dB.

It is immediately seen from the entries in Table 1 that, indeed, the false alarm probability in the presence of interference, but in the absence of the suppression filter, can be so large as to make the system useless. However, when the interference suppression filter is inserted into the system, the false alarm probability is reduced to an acceptable level.

V. Other Interference Rejection Structures

The previous sections have emphasized two specific techniques for interference rejection, one employing the estimation-type filter and the other making use of transform domain processing ideas. These two interference suppression techniques were chosen in part because of the familiarity of the author with them and in part because they happen to be generating interest outside of just the academic/research community. However, a variety of other rejection schemes have been proposed and some of these are briefly described below.

If the interference is both sufficiently narrowband and sufficiently strong to allow a phase-locked loop (PLL) to

achieve phase-lock on it in the presence of the desired signal and thermal noise, it is possible to form a composite estimate (i.e., one accounting for both phase and amplitude) of the interference and subtract it from the received waveform. While the idea of subtracting an estimate from the received signal sounds similar to the method described in Section II, the manner in which the estimate is obtained is quite different.

One system designed to reject interference as just described is presented in [6], and a block diagram of the receiver is shown in Fig. 31. The ratio of interference power
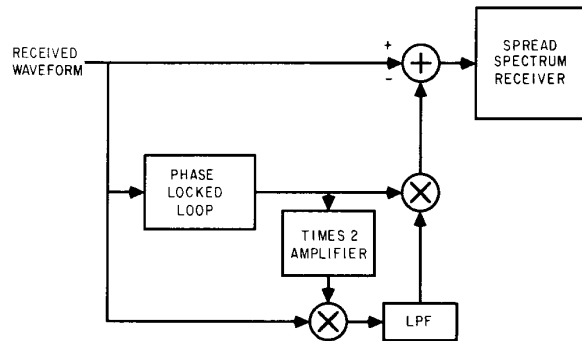

Fig. 31. Rejection scheme of [6].

to signal power is assumed large enough so that the PLL locks onto the frequency and phase of the interference. Again, because of the relatively large interference level, the amplitude of the output of the low pass filter shown in the lower arm of the receiver of Fig. 31 is dominated by the interference. Hence the locally generated reference to the subtractor in the upper arm becomes the desired estimate of the interference. In [35], a technique similar to that of [6] is presented, but with the addition of various circuitry designed to result in a more accurate estimate of the interference than is achieved in [6].

A technique for canceling wide-band interference is described in [5]. Referring to Fig. 32, it is seen that if the ratio of interference power-to-signal power is sufficiently large, the output of the limiter is essentially the interference. However, the output of amplifier 1 consists of both signal plus interference, meaning that if the gain can be appropriately adjusted, the difference circuit can be used to suppress the interference. This gain adjustment is accomplished by an AGC operation.
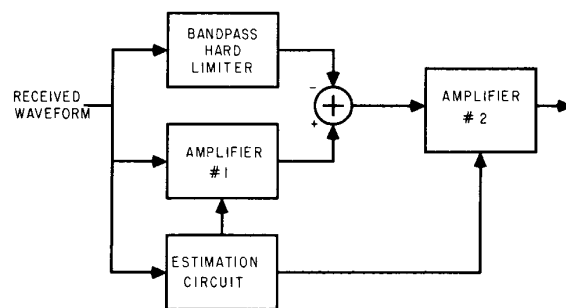

Fig. 32. Rejection scheme of [5].

The analyses presented in [6], [35], [5] correspond to noise-free conditions. Hence, it appears to be an open question as to how well these techniques perform in the very low signal-to-(thermal) noise ratio environment typical of most spread spectrum receivers.

A completely different technique for making a DS receiver more robust with respect to interference is described in [2], [3], [40]. This scheme uses an A/D converter, in conjunction with a variable threshold, to retain those chips of the spreading sequence which, when added to a strong interfering signal, are still received with their correct polarity. For this system to operate properly, it is necessary to have both a large J/S and a large ratio of interference power-to-noise power.

CONCLUSIONS

In this paper, a variety of interference suppression schemes designed to operate in conjunction with a DS spread spectrum receiver were described. Emphasis was placed on two general techniques, one using Wiener-type filters and the other employing transform domain processing. Both techniques were shown to have the potential of yielding a sizable improvement in system performance relative to that achievable by a conventional DS receiver, but that the improvement was subject to certain constraints.

Most notably was the constraint that the interference be relatively narrowband with respect to the DS waveform. Also, since high-speed signal processing is inherent in virtually any DS system, implementation of these schemes is limited to certain wide-band technologies such as SAW and CCD, and these technologies, in turn, have certain limitations such as dynamic range.

Regarding which scheme to use in a given scenario, it appears that each one has its own set of advantages and disadvantages. To see this, consider the simple example of a sinewave interferer at a known frequency. Whereas the estimation-type filter can, if desired, put a zero at the frequency of the sinewave and hence null it out completely, this complete nulling is typically not possible for the TDP receiver. Because the input to the TDP receiver is windowed in time before it is Fourier transformed, sidelobes are immediately put on the interference spectrum and, hence, even an infinitely deep notch over some appropriate fraction of the bandwidth of the system will not completely eliminate the interference. Alternately, because the TDP system can be made adaptive on an essentially "instantaneous" basis, without the need for an adaptive algorithm with its attendant convergence problems, the TDP receiver would seem to have an advantage over the receiver employing an estimation filter in those scenarios whereby rapid adaptivity is required.

There is still much to be learned in the area of interference rejection and this remains an active research field. In addition to the specific topics mentioned in this paper, other current areas of research include the use of interference suppression schemes to aid in the initial acquisition of the DS signal and the use of such techniques in a spread spectrum network.

ACKNOWLEDGMENT

The author wishes to thank Prof. R. Rao for carefully reading the manuscript and making some useful suggestions on improving the presentation of the material.

REFERENCES

[1] S. T. Alexander, Adaptive Signal Processing. New York, NY: Springer-Verlag, 1986.
[2] F. Amoroso, "Adaptive A/D converter to suppress CW interference in DSPN spread-spectrum communications," IEEE Trans. Commun., vol. COM-31, pp. 1117-1123, Oct. 1983.
[3] F. Amoroso and J. L. Bricker, "Performance of the adaptive A/D converter in combined CW and gaussian interference," IEEE Trans. Commun., vol. COM-34, pp. 209-213, Mar. 1986.
[4] C. Atzeni, G. Manes, and L. Masotti, "Programmable signal processing by analog chirp transformation using SAW devices," in Proc. 1975 Ultrasonics Symp., p. 572, 1973.
[5] P. W. Baier and K. J. Friederichs, "A nonlinear device to suppress strong interfering signals with arbitrary angle modulation in spread-spectrum receivers," IEEE Trans. Commun., vol. COM-33, pp. 300-302, Mar. 1985.
[6] M. J. Bouvier, Jr., "The rejection of large CW interferers in spread spectrum systems," IEEE Trans. Commun., vol. COM-28, pp. 254-256, Feb. 1978.
[7] J. H. Cafarella, W. M. Brown, Jr., E. Stern, and J. A. Alusow, "Acoustoelectric convolvers for programmable matched filtering in spread-spectrum system," Proc. IEEE, vol. 64, p. 756, 1976.
[8] P. Das, L. B. Milstein, and R. T. Webster, "Application of SAW chirp transform filter in spread spectrum communication systems," in 6th European Microwave Conf., pp. 261-266, Sept. 1976.
[9] A. Gersho, "Charge coupled devices: The analog shift register comes of age," IEEE Commun. Mag., pp. 27-32, Nov. 1975.
[10] J. Gevargiz, M. Rosenmann, P. Das, and L. B. Milstein, "A comparison of weighted and nonweighted transform domain processing systems for narrowband interference excision," in IEEE Military Communications Conf., pp. 32.3.1-32.3.4, Oct. 1984.
[11] J. Gevargiz, P. Das, and L. B. Milstein, "Implementation of a transform domain processing radiometer for DS spread spectrum signals with adaptive narrowband interference exciser," presented at the IEEE International Conf. on Communications, June 1985.
[12] J. Gervargiz, P. Das, L. B. Milstein, J. Moran, and O. McKee, "Implementation of DS-SS intercept receiver with an adaptive narrowband interference exerciser using transform domain processing and time weighting," in IEEE Military Communications Conf., pp. 20.1.1-20.1.5, Oct. 1986.
[13] J. Gevargiz, P. Das, and L. B. Milstein, "Performance of a transform domain processing DS intercept receiver in the presence of finite bandwidth interference," in IEEE Global Telecommunications Conf., pp. 21.5.1-21.5.5, Dec. 1986.
[14] A. A. Giordano and F. M. Hsu, Least Square Estimation with Applications to Digital Signal Processing. New York, NY: Wiley-Interscience, 1985.
[15] J. Guilford and P. Das, "The use of the adaptive lattice filter for narrowband jammer rejection in DS spread spectrum systems," in Proc. IEEE International Conf. on Communications, pp. 822-826, June 22-26, 1985.
[16] C. W. Helstrom, Statistical Theory of Signal Detection. New York, NY: Pergamon, 1960.
[17] F. M. Hsu and A. A. Giordano, "Digital whitening techniques for improving spread-spectrum communications performance in the presence of narrow-band jamming and interference," IEEE Trans. Commun., vol. COM-26, pp. 209-216, Feb. 1978.
[18] R. A. Iltis and L. B. Milstein, "Performance analysis of narrowband interference rejection techniques in DS spread-spectrum systems," IEEE Trans. Commun., vol. COM-26, pp. 209-216, Feb. 1978.
[19] ——, "An approximate statistical analysis of the Widrow LMS algorithm with application to narrow-band interference rejection," IEEE Trans. Commun., vol. COM-33, pp. 121-130, Feb. 1985.
[20] J. W. Ketchum and J. G. Proakis, "Adaptive algorithms for estimating and suppressing narrow-band interference in PN spread-spectrum systems," IEEE Trans. Commun., vol. COM-30, pp. 913-924, May 1982.
[21] J. W. Ketchum, "Decision feedback techniques for interference cancellation in PN spread-spectrum communication systems," in IEEE Military Communications Conf., pp. 39.5.1-39.5.5, Oct. 1984.

[22] L. Li and L. B. Milstein, "Rejection of narrow-band interference in PN spread-spectrum systems using transversal filters," *IEEE Trans. Commun.*, vol. COM-30, pp. 925–928, May 1982.

[23] ——, "Rejection of CW interference in QPSK systems using decision-feedback filters," *IEEE Trans. Commun.*, vol. COM-31, pp. 473–483, Apr. 1983.

[24] Z. Li, H. Yuan, and G. Bi, "Rejection of multi-tone interference in PN spread spectrum systems using adaptive filters," in *IEEE International Conf. on Communications*, pp. 24.5.1–24.5.5, June 1987.

[25] F. Lin and L. M. Li, "Rejection of finite-bandwidth interference in QPSK systems using decision-feedback filters," in *IEEE International Conf. on Communications*, pp. 24.6.1–24.6.5, June 1987.

[26] E. Masry, "Closed-form analytical results for the rejection of narrow-band interference in PN spread-spectrum systems—Part I: Linear prediction filters," *IEEE Trans. Commun.*, vol. COM-32, pp. 888–896, Aug. 1984.

[27] ——, "Closed-form analytical results for the rejection of narrow-band interference in PN spread-spectrum systems—Part II: Linear interpolation filters," *IEEE Trans. Commun.*, vol. COM-33, pp. 10–19, Jan. 1985.

[28] E. Masry and L. B. Milstein, "Performance of DS spread-spectrum receivers employing interference-suppression filter under a worst-case jamming condition," *IEEE Trans. Comm.*, vol. COM-34, pp. 13–21, Jan. 1986.

[29] L. B. Milstein and P. Das, "Spread spectrum receiver using acoustic surface wave technology," *IEEE Trans. Commun.*, vol. COM-25, no. 8, pp. 841–847, Aug. 1977.

[30] ——, "Surface acoustic wave devices," *IEEE Commun. Mag.*, pp. 25–33, Sept. 1979.

[31] ——, "An analysis of a real-time transform domain filtering digital communication system, Part I: Narrowband interference rejection," *IEEE Trans. Commun.*, vol. COM-28, pp. 816–824, June 1980.

[32] L. B. Milstein, P. K. Das, and J. Gevargiz, "Processing gain advantage of transform domain filtering DS spread spectrum systems," *Military Communications Conf.*, pp. 21.2.1–21.2.4, Oct. 1982.

[33] L. B. Milstein and P. K. Das, "An analysis of a real-time transform domain filtering digital communication system—Part II: Wideband interference rejection," *IEEE Trans. Commun.*, vol. COM-31, pp. 21–27, Jan. 1983.

[34] L. B. Milstein and R. A. Iltis, "Signal processing for interference rejection in spread-spectrum communications," *IEEE ASSP Mag.*, pp. 18–31, Apr. 1986.

[35] A. E. S. Mostafa, M. Abdel-Kader, and A. El-Osmany, "Improvements of anti-jam performance of spread-spectrum systems," *IEEE Trans. Commun.*, vol. COM-31, pp. 803–808, Jan. 1983.

[36] G. R. Nudd and O. W. Otto, "Chirp signal processing using acoustic surface wave filters," in *1975 Ultrasonics Symp. Proceedings*, p. 350, 1975.

[37] J. Ogawa, S. J. Cho, N. Morinaga, and T. Namekawa, "Optimum detection of *M*-ary PSK signal in the presence of CW interference," *Trans. IECE Japan*, vol. E64, pp. 800–806, Dec. 1981.

[38] O. W. Otto, "Real-time Fourier transform with a surface wave convolver," *Electron Lett.*, vol. 8, p. 623, 1972.

[39] A. Papoulis, *Probability, Random Variables and Stochastic Processes.* New York, NY: McGraw-Hill, 1965, pp. 218–220.

[40] F. J. Pergal, "Adaptive threshold A/D conversion techniques for interference rejection in DSPN receiver applications," in *IEEE Military Communications Conf.*, pp. 4.7.1–4.7.7, Oct. 1987.

[41] R. L. Pickholtz, D. L. Schilling, and L. B. Milstein, "Theory of spread-spectrum communications—a tutorial," *IEEE Trans. Commun.*, vol. COM-30, pp. 855–884, May 1982.

[42] J. G. Proakis, *Digital Communications.* New York, NY: McGraw-Hill, 1983.

[43] M. Rosenmann, M. J. Gevargiz, P. K. Das, and L. B. Milstein, "Probability of error measurement for an interference resistant transform domain processing receiver," in *IEEE Military Communications Conf.*, pp. 638–640, Oct. 1983.

[44] G. I. Saulnier, P. Das, and L. B. Milstein, "Suppression of narrow-band interference in a PN spread-spectrum receiver using a CTD-based adaptive filter," *IEEE Trans. Commun.*, vol. COM-32, pp. 1227–1232, Nov. 1984.

[45] ——, "An adaptive digital suppression filter for direct-sequence spread-spectrum communications," *IEEE J. Selected Areas Commun.*, vol. SAC-3, no. 5, pp. 676–686, Sept. 1985.

[46] ——, "Suppression of narrow-band interference on a direct sequence spread spectrum receiver in the absence of carrier synchronization," in *IEEE Military Communications Conf.*, pp. 13–17, Oct. 1985.

[47] G. J. Saulnier, K. Yum, and P. Das, "The suppression of tone jammers using adaptive lattice filtering," in *IEEE International Conf. on Communications*, pp. 24.4.1–24.4.5, June 1987.

[48] D. Shklarsky, P. K. Das, and L. B. Milstein, "Adaptive narrowband interference suppression," in *1979 National Telecommunications Conf.*, pp. 15.2.1–15.2.4, Nov. 1979.

[49] M. K. Simon, J. Omura, R. A. Scholtz, and B. K. Levitt, *Spread-Spectrum Communications*, vols. I–III. Rockville, MD: Computer Science Press, 1985.

[50] F. Takawira and L. B. Milstein, "Narrowband interference rejection in PN spread spectrum systems using decision feedback filters," in *IEEE Military Communications Conf.*, pp. 20.4.1–20.4.5, Oct. 1986.

[51] Y.-C. Wang and L. B. Milstein, "Rejection of multiple narrowband interference in both BPSK and QPSK DS spread-spectrum systems," *IEEE Trans. Commun.*, vol. COM-36, pp. 195–204, Feb. 1988.

[52] B. Widrow et al., "Adaptive noise canceling: Principles and applications," *Proc. IEEE*, vol. 63, pp. 1692–1716, Dec. 1975.

[53] B. Widrow and S. D. Stearns, *Adaptive Signal Processing.* Englewood Cliffs, NJ: Prentice-Hall, 1985.

[54] R. E. Ziemer and R. L. Peterson, *Digital Communications and Spread Spectrum.* New York, NY: MacMillan, 1985.

Laurence B. Milstein (Fellow, IEEE) received the B.E.E. degree from the City College of New York, New York, NY, in 1964, and the M.S. and Ph.D. degrees in electrical engineering from the Polytechnic Institute of Brooklyn, Brooklyn, NY, in 1966 and 1968, respectively.

From 1968 to 1974 he was employed by the Space and Communications Group of Hughes Aircraft Company, and from 1974 to 1976 he was a member of the Department of Electrical and Systems Engineering, Rensselaer Polytechnic Institute, Troy, NY. Since 1976 he has been with the Department of Electrical and Computer Engineering, University of California at San Diego, La Jolla, where he is a Professor and Department Chairman, working in the area of digital communication theory with special emphasis on spread-spectrum communication systems. He has also been a consultant to both government and industry in the areas of radar and communications.

Dr. Milstein was an Associate Editor for Communication Theory for the IEEE TRANSACTIONS ON COMMUNICATIONS and an Associate Technical Editor for the IEEE COMMUNICATIONS MAGAZINE. He was a member of the Board of Governors of the IEEE Communications Society, and is a member of Eta Kappa Nu, Tau Beta Pi, and Sigma Xi.